

Stapp Car Crash Journal 44 (November 2000) 189-204 Copyright © 2000 The Stapp Association

# Biomechanics of Human Occupants in Simulated Rear Crashes: Documentation of Neck Injuries and Comparison of Injury Criteria

Narayan Yoganandan, Frank A. Pintar, Brian D. Stemper, Michael B. Schlick

Department of Neurosurgery
Medical College of Wisconsin and VA Medical Center

Mat Philippens, Jac Wismans
TNO Automotive

## **ABSTRACT**

The objective of this study was to subject small female and large male cadavers to simulated rear impact, document soft-tissue injuries to the neck, determine the kinematics, forces and moments at the occipital condyles, and evaluate neck injury risks using peak force, peak tension and normalized tension-extension criteria. Five unembalmed intact human cadavers (four small females and one large male) were prepared using accelerometers and targets at the head, T1, iliac crest, and sacrum. The specimens were placed on a custom-designed seat without head restraint and subjected to rear impact using sled equipment. High-speed cameras were used for kinematic coverage. After the test, x-rays were obtained, computed tomography scans were taken, and anatomical sections were obtained using a cryomicrotome. Two female specimens were tested at 4.3 m/s (mean) and the other two were tested at 6.8 m/s (mean), and one large male specimen was subjected to 6.6 m/s velocity. One female specimen tested at 4.1 m/s did not sustain injury. All others produced injuries to soft tissue and joint-related structures that included tearing of the anterior longitudinal ligament, rupture of the ligamentum flavum, hematoma at the upper facet joint, anterior disc disruption at the lower spine, and facet joint capsule tear. Compressive forces (100 to 254 N) developed within 60 ms after impact. Tensile forces

were higher (369 to 904) and developed later (149 to 211 ms). While peak shear forces (268 to 397 at 4.3 m/s and 257 to 525 N at 6.8 m/s) did not depend on velocity, peak tensile forces (369 to 391 N at 4.3 m/s and 672 to 904 N at 6.8 m/s) seemed to correlate with velocity. Peak extension moments ranged from 22.0 to 33.5 Nm at low velocity and 32.7 to 46.6 Nm at high velocity. All these biomechanical data attained their peaks in the extension phase (with very few exceptions), which ranged from 179 to 216 ms. The neck injury criterion, NIC, exceeded the suggested limit of 15 m<sup>2</sup>/s<sup>2</sup> in all specimens. Axial force and bending moment data were used to evaluate various neck injury criteria (Nij, NTE, peak tension and peak extension). The risk for AIS  $\geq 3$ injury for the combined tension-extension criteria was 30 percent in one female specimen tested at 6.8 m/s. For the other specimens the risk of AIS  $\geq 3$ injury was less than five percent using all criteria.

# INTRODUCTION

Biomechanics of the human occupant in rear impacts has been investigated since the 1950s [1]. Mertz and Patrick conducted early research [2]. Human volunteers, human cadavers, and dummies were used as experimental models in their tests. The extension bending moment tolerance of 57 Nm for the 50<sup>th</sup> percentile adult male was obtained using rear impact tests of two male cadavers from the study [2]. One

male human cadaver sustained minor ligamentous damage between the third and fourth cervical vertebrae and no damage was observed for the other male cadaver. These cadavers were tested at 4.0 and 6.8 m/s changes in velocity. Since this well-cited study, to the best of our knowledge, unembalmed human cadaver studies have not been conducted that documented injuries to the head-neck structures. quantified biomechanical parameters, and evaluated injury criteria. There is a paucity of these data to cover the range of vehicle occupants, i.e., from small female to large male. The focus of the present research is, therefore, to subject small female and large male intact human cadavers to simulated rear impact, document injuries to the hard and soft tissue cervical structures, determine the forces and moments at the occipital condyles, and determine neck injury risk using proposed injury criteria.

# MATERIALS AND METHODS

SPECIMEN SELECTION - Five unembalmed human cadavers were used in the study (4 female, 1 male). Details of the subjects (called specimens) are given in table A. Pretest anthropometric data were taken. Mass and moment of inertia of the head were calculated using head geometrical dimensions and regression equations given by McConville et al [3]. In previous studies presented at Stapp conferences, Wismans et al and Kroonenberg et al adopted a similar procedure [4, 5]. Table A includes these data on a specimen-by-specimen basis. In addition, pretest x-rays of the head and neck structures were obtained in the lateral and antero-posterior planes. The subjects were clothed in close-fitting cotton leotards and placed on a custom-designed seat.

SEAT DESIGN - The seat was fabricated from steel such that the seat panel (where the pelvis and upper portion of the lower extremities rest) was inclined 10 degrees (Figure 1). The seat back, which provides support for the torso region, was inclined rearward by an angle of 114 degrees from the horizontal plane (x-axis). The seat panel measured 448 mm x 400 mm. The seat back measured 448 mm x 700 mm for male and 448 mm x 583 mm for female specimens. The height of the seat at the intersection of the seat back and seat panel was 155 mm. The seat was rigidly attached to the base of the sled at the four corners of the seat panel. In addition, two parallel struts to prevent rearward motion of the seat structure braced the seat back. The struts were also

rigidly attached to the base of the sled. The seat back was slotted at the top and bottom to permit documentation of the specimen kinematics (Figure 1). A cushion consisting of 38 mm of foam was placed on the seat back in some tests. The seat was fixed to the deceleration sled, which induced rear impact acceleration to the test specimen.

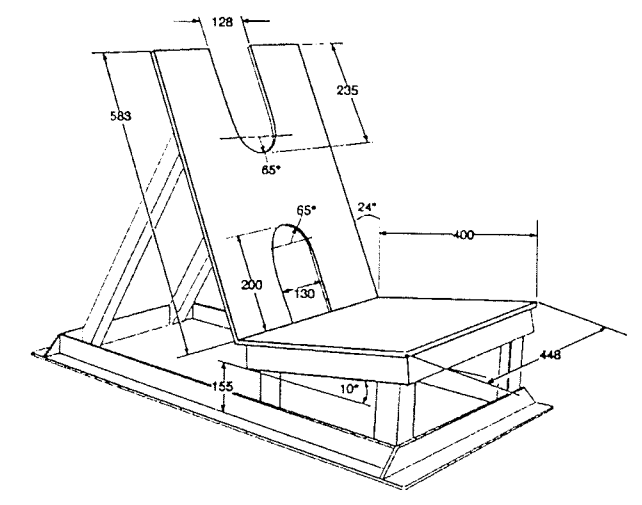


Figure 1: Seat used in rear impact tests.

POSITIONING OF THE SPECIMEN - The leotard-clothed specimen was placed on the seat such that the knee-foot-ankle region of the lower extremities was stretched out. The head Frankfort plane was horizontal and the two upper extremities crossed in front of the thorax. The torso was restrained by a three-point belt. The lap belt was tightened without allowing slack and custom cinch plates were used to lock the restraint. A restraint was used to position the head prior to impact; this positioning device swung out of the way due to an inertial mechanism during impact. Radiographs of the specimen were taken in this position prior to impact acceleration.

INSTRUMENTATION AND PHOTOGRAPHY - Triaxial linear accelerometers were fixed to the vertex of the skull, spinous process of the first thoracic vertebra, sacrum, and sled (Figure 2). A triaxial angular velocity sensor was attached to the head. Photographic documentation and analysis of the impact test were accomplished using targets attached to the specimen-based accelerometers (Figure 3), seat back and seat panel, and the sled. The impact event was documented using high-speed photography. Overall right lateral, overhead top, close-up lateral head-neck, and close-up lateral neck-torso-pelvis views were taken at 1000 f/sec (Figure 4).

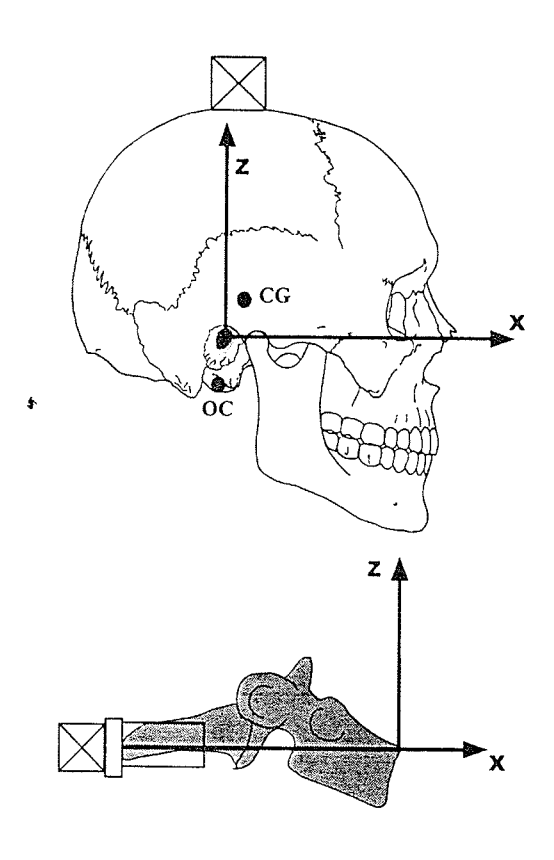


Figure 2: Schematic of specimen with accelerometer instrumentation at the head (top) and spinous process of T1 vertebra (bottom). The location of anatomical origin is shown. OC and CG locations are shown to illustrate their approximate positions.

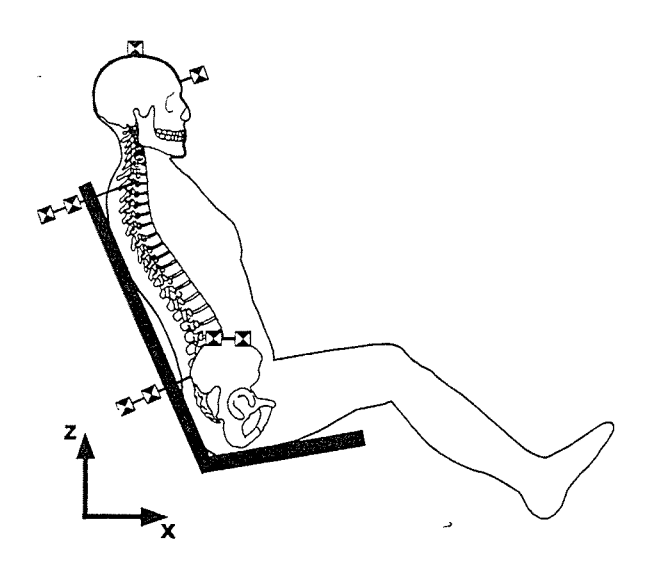


Figure 3: Schematic of the photographic targets at the head, dorsal spine and iliac crest. The laboratory coordinate system is indicated in the bottom lefthand corner.

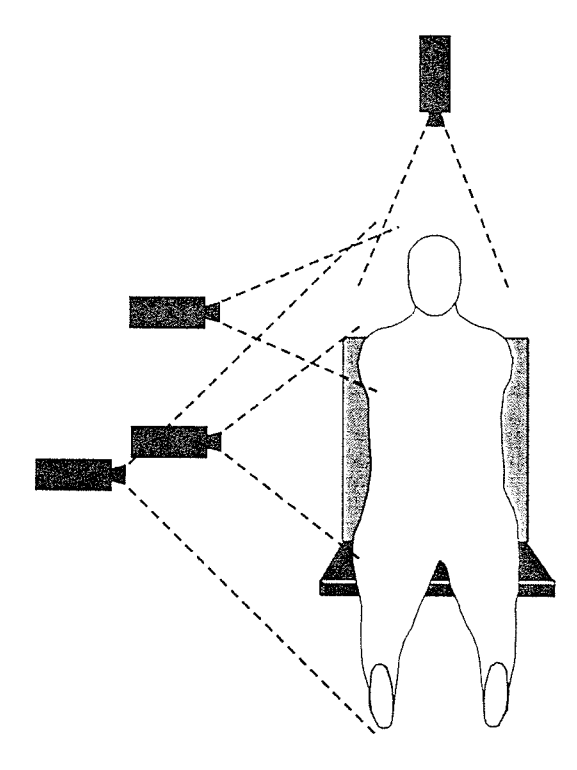


Figure 4: Positioning of the three onboard highspeed cameras for right side views and an overhead camera for top view. The left side and oblique view cameras are not shown.

BIOMECHANICAL DATA - For computational purposes, three coordinate systems were defined: accelerometer/sensor, anatomical (Figure 2), and laboratory (Figure 3). The local coordinate system of the accelerometer was defined at the center of gravity (cg) of the sensor array. The anatomical coordinate system of reference was defined for each body region. The right hand Cartesian coordinate system of reference was used with the local x-axis directed anteriorly from the anatomical origin, local y-axis directed from right to left (from the origin), and local z-axis directed superiorly from the origin. Landmarks that defined the head anatomical system were such that the origin was located in the midsagittal plane between the left and right auditory meatii. Landmarks that defined the T1 anatomical system were such that the origin was located at the superior-anterior tip of the vertebral body. For the pelvis, landmarks that defined the anatomical coordinate system were such that the origin was at the superior aspect of the pubic symphysis. Pretest radiographs were used to document the anatomical landmarks. The specimens were tested once using the sled equipment. The velocities were set at either 4.1 or 6.9 m/s.

IMAGING - After the rear impact test, x-rays and computed tomography (CT) images of the head-neck complex were obtained at close-up 1.0-mm intervals. Sequential anatomical sections were obtained using a heavy-duty cryomicrotome at intervals of 15 to 30 microns. Overall and close-up color photographs of cryosections depicting the hard and soft tissues were taken to identify structural alterations. Data were compared with x-ray and CT information to provide a comprehensive assessment of cervical injury to each specimen.

DATA ANALYSIS - Methods used to analyze the response of the human surrogates from experimental data are described in earlier Stapp literature [2, 4, 5]. The basic method and equations used by Wismans et al were used in the present study assuming the head as a rigid body with no head contact and pure sagittal plane motion [5]. The neck reaction loads were obtained at the occipital condyles using classic mechanics equations of dynamic equilibrium. Data from sensors were sampled at a frequency of 12.5 kHz and filtered according to the Society of Automotive Engineers (SAE) specifications. Headneck motions were determined. Photographic target trajectories (x and z displacements) were obtained by digitizing every frame from high-speed films. The resulting raw target coordinates were smoothed using a third-order spline function. Positions of the head and T1 anatomical origins were expressed in a laboratory-related sled coordinate system (Figure 3). Positions of the anatomical origins with respect to the photographic targets were obtained from pretest x-rays. The x and z coordinates of the cg of the head were determined using a standard cg location with respect to the anatomical coordinates determined for each specimen [6]. Laboratory-related x and z coordinates of the occipital condyles were determined from x-rays with respect to the anatomical origin of the head.

Linear accelerations at the cg of the head with respect to the head anatomical coordinate system were computed using measured linear acceleration and angular velocity data recorded at the vertex of the head (Figure 2). Angular velocity data were differentiated to obtain time-dependent angular acceleration information. Positions of the sensors with respect to the corresponding anatomical origin were derived from pretest x-rays. Linear accelerations of the anatomical origin of T1 were assumed to be equal to the measured linear

accelerations at the spine. In other words, the angular acceleration of the T1 vertebra was neglected. Normal and shear forces and bending moments at the occipital condyles were computed using linear and angular acceleration data of the cg of the head and employing the dynamic equations of equilibrium.

#### RESULTS

Table A provides a summary of all data on a specimen-by-specimen basis. Figure A illustrates the sled pulse, head cg x and z accelerations, head angular acceleration, head extension angle, T1 x and z accelerations, head x and z displacements, and occipital condylar axial and shear forces and bending moment data for specimen 104. Data are split into extension and rebound phases. A vertical line drawn in the plot indicates the end of the extension phase, which was defined to begin from tzero and culminating at the time when the head was in maximum extension. The rebound phase commenced following the end of the extension phase.

TEST MATRIX - The measured change in velocity ranged from 4.14 to 6.89 m/s with average sled accelerations ranging from 32.4 to 46.1 m/s<sup>2</sup>. Three specimens (101, 104, 105) were tested at high (6.6 to 6.9 m/s) and two specimens (102, 103) were tested at low (4.1 and 4.4 m/s) velocities. Three specimens were seated using a cushion and the other two did not use a cushion. All specimens were belted; in the first specimen however, the belt was not tightened at the cinch plate.

X-RAY DATA - The anatomical landmarks of the inferior orbit, occipital condyles and T1 obtained from x-rays are given in table A. Standard x and z coordinates of the cg of the head with respect to the anatomical origin were taken as 8.3 and 31 mm (y = 0), respectively, for all specimens. This procedure was adopted in the present study since no additional experiments were conducted to separately determine the cg of the head for each tested specimen. However, it should be noted that while previous research by Wismans and Spenny, and Wismans et al used the same anatomical condyle location for all their subjects, these data were specimen dependent in the present study [5, 7].

MEASURED ACCELERATION - The maximum values of measured acceleration at the vertex of the head are not reported since the orientations of the accelerometer array were different for each specimen, and consequently, processed cg head accelerations are given. The T1 accelerometer array was mounted quite consistently to be oriented to align with the T1 anatomical coordinate system (Figure 2) and, therefore, the data can be reasonably compared. Maximum positive x accelerations were consistently greater than the negative x accelerations. Using a SAE J211 class 180 filter, maximum positive x accelerations ranged from 82.9 to 132.8 m/s<sup>2</sup> in the extension phase. The z accelerations did not demonstrate any noticeable pattern of consistency and peak magnitudes ranged from 20.4 to 79.8 m/s<sup>2</sup> in the extension phase (Table A).

HEAD ROTATIONS - The maximum extension of the head ranged from 123 to 149 degrees for all specimens. The time of occurrence of peak extensions ranged from 179 to 216 ms. The head rotation began to increase 75 to 103 ms after the initiation of sled deceleration with the exception of specimen 105 wherein the rotation initiated after 30 ms. After the attainment of peak head rotational extension, the specimen began to rebound. The time of maximum rotational extension defined the end of the extension phase and beginning of the rebound phase.

HEAD DISPLACEMENTS - In the extension phase, peak head x displacements with respect to T1 ranged from 0.08 to 0.16 m (along the anterior to posterior direction). Peak z displacements (positive) ranged from 0.01 to 0.03 m. This was followed by negative z displacements that ranged from 0.04 to 0.09 m.

LINEAR ACCELERATIONS AT THE CG OF THE HEAD - In the extension phase, peak posterior-to-anterior (positive x-axis) accelerations ranged from 61.6 to 95.1 m/s<sup>2</sup> and peak anterior-to-posterior accelerations (negative x-axis) ranged from 75.5 to 86.0 m/s<sup>2</sup>. Peak accelerations in this phase ranged from 62.5 to 152.1 m/s<sup>2</sup> along the superior-to-inferior direction (negative z-axis) and 9.7 to 48.4 m/s<sup>2</sup> along the inferior-to-superior (positive z-axis) direction. All positive and negative x and z accelerations reached their respective maximum values in the extension phase with the exception of peak positive x and z accelerations in specimen 101.

and the peak positive x acceleration in specimen 102. Peak positive z accelerations preceded peak positive x accelerations in all specimens. In addition, peak negative x accelerations preceded peak positive x accelerations for all except specimen 102 (Table A).

HEAD ANGULAR ACCELERATIONS - Peak angular accelerations ranged from 590 to 1200 rad/sec² in the extension phase. These were also the absolute maximum accelerations for all specimens with the exception of specimen 101 in which a value of 1310 rad/sec² was recorded in the rebound phase. This was most likely due to the breaking of the sled in the later stages of rebound, which only occurred in this test. The peak head angular accelerations were recorded in specimen 104 which had the highest body and head mass.

FORCES AT THE OCCIPITAL CONDYLES - During the extension phase, peak shear forces ranged from 257 to 525 N and peak compressive forces ranged from 100 to 254 N. Maximum compressive forces developed early in the rear impact (with in the first 61 ms). In contrast, peak shear forces developed later. Peak tensile forces (369 to 904 N) were higher and occurred later (149 to 211 ms) than peak compressive forces. In the rebound phase, shear and axial forces were smaller for all specimens except the first two (101 and 102), wherein shear forces were only slightly higher (378 and 397 N).

When forces were categorized into the two groups of changes in velocity, for the low-velocity runs, shear forces ranged from 268 to 397 N and axial compressive forces ranged from 100 to 119 N. At high velocity, shear and compressive forces ranged from 257 to 525 N and 132 to 254 N, respectively. Peak tension force seemed to be more dependent on velocity with ranges from 369 to 391 N and 672 to 904 N for the low and high velocities, respectively.

BENDING MOMENT AT THE OCCIPITAL CONDYLES - Peak extension bending moments at the occipital condyles ranged from 22 to 46.6 Nm in the extension phase. The time of occurrence of these moments ranged from 173 to 200 ms. These time periods were at or near the time of maximum extension of the head, i.e., end of the extension phase. In the rebound phase, the magnitudes of these moments were all lower than in the extension

phase with the exception of specimen 102 wherein a slightly higher moment occurred. Therefore, in general, maximum extension bending moments developed during the initial extension phase of rear impact acceleration. When data were categorized on the basis of changes in velocity, extension moments ranged from 22.0 to 33.5 Nm for low- and 32.7 to 46.6 Nm for high-velocity tests.

INJURY DOCUMENTATION - When pathology was categorized based on change in velocity, out of the two specimens (102, 103) subjected to low changes in velocity (4.1 to 4.4 m/s), only one (103) sustained injuries (Figure 5). In specimen 103, trauma included a widening of the facet joint at the C5-6 level on the right side with a ligamentum flavum tear at the next adjacent inferior level. All three specimens subjected to higher changes in velocity (6.6 to 6.9 m/s) sustained injuries to the soft tissues and joints of the cervical structures. Injuries included the following. Specimen 101 sustained a tear in the C5-6 disc with a rupture of the flavum at the C6-7 level. Specimen 104 demonstrated widening and disruption of the C5-6 facet joint on the right, and widening of the left C4-5 facet joint and stretch of the C5-6 capsule, together with rupture of the anterior longitudinal ligament at C5-6 accompanied by a disc tear. Specimen 105 sustained a chip fracture of the fifth vertebral body, accompanied by hematoma in the right C5-6 and left C1-2 facet joints.

NECK INJURY CRITERIA - The newly proposed neck injury criterion, Nij, was computed using the procedures outlined by Eppinger et al [8]. Since the cadavers used in the present study were close to the 5<sup>th</sup> female (specimens 101, 102, 103, 105) and 95<sup>th</sup> male (specimen 104) anthropometry, recommended intercept values for these standard sizes were used to derive N<sub>ij</sub> values [9,10]. In all specimens, peak tension and compression forces did not exceed tolerance limits (Table 1). Specifically, tension did not exceed 35 percent and compression did not exceed 12 percent of the proposed values (Table A). All Nij values reached their maximum in the extension phase (Table A) and they ranged from 0.2 to 1.3 with an associated risk ranging from 0 to 22 percent. The neck injury criterion (NIC) proposed by Bostrom et al ranged from 19.2 to 37.0 m<sup>2</sup>/s<sup>2</sup> (Table A) [11]. The suggested limit of 15 m<sup>2</sup>/s<sup>2</sup> exceeded in all specimens.

Table 1a: Out-of-Position Intercept Values for N<sub>ij</sub> [9,10]

Intercept	5 <sup>th</sup> Female	95 <sup>th</sup> Male
Tension (N)	3880	7440
Extension (Nm)	61	162
Compression (N)	3880	7440
Flexion (Nm)	155	415

Table 1b: Out-of-Position Peak Tension and Compression

Condition	5 <sup>th</sup> Female	95 <sup>th</sup> Male
Tension (N)	2070	3970
Compression (N)	2520	4830

Where  $N_{ij} = F/F_1 + M/M_1$ 

Subscript I denote the intercept value, and F and M denote force and moment data. N<sub>ij</sub> denotes the injury index.

Ocipital condyle force and moment data were also used to evaluate other injury criteria (Table 2) suggested by Mertz et al [12]. The peak tension force in each specimen (Table A, forces at occipital condyles) did not exceed proposed limits shown in table 2. The maximum bending moment also did not exceed proposed limits in specimens 102 and 104 (Table A, moments at occipital condyles). The peak moment, however, exceeded the suggested limit in the other three specimens.

Normalized tension  $(F_T)$  did not exceed the critical value of 1.0 in all specimens in the present study. The maximum associated neck injury risk at the AIS  $\geq$  3 level was less than 0.1 percent. However, calculated normalized extension values  $(M_E)$  for female specimens exceeded suggested limits in three out of four specimens (Table A). The risk of AIS  $\geq$  3 neck injury, determined using the risk lines provided by Mertz et al, ranged from two to four percent for these data. However, for the large male specimen, the extension limit was not exceeded indicating no risk of AIS  $\geq$  3 injury.

The injury index,  $N_{TE}$ , under combined extension-tension mode, ranged from 0.71 to 2.27 for female specimens and was 0.57 for the male specimen (104). The risk of AIS  $\geq$  3 injury was determined to be less than five percent for all specimens except specimen 105, which resulted in a 30 percent risk of injury to the neck.

Table 2: Various Proposed Limits for Neck Injury [12]

Parameter	5 <sup>th</sup> Female	95 <sup>th</sup> Male
Tension (N)	2200	4050
Extension (Nm)	31	78
Tension intercept (N) for	1660	3190
normalized neck tension		
Extension intercept (Nm) for	25	67
normalized extension		
Combined tension-extension $N_{TE}$		
Tension intercept (N)	2470	4730
Extension intercept (Nm)	39	103

The AIS  $\geq$  3 injury risk was obtained using the normal distribution functions representing risk versus normalized force/moment data provided by Mertz et al. Indices  $F_T$ ,  $M_E$ ,  $N_{TE}$ , were computed using the following equations. The intercept values were set at one percent level of AIS  $\geq$  3 neck injury for the condition of minimum muscle tone.

 $F_T = F_E / F_I$ ;

 $M_E = M_E / M_I$ ; and

 $N_{TE} = F_T/F_I + M_E/M_I$ 

Subscripts E, T and I denote extension, tension, and intercept; F, M and N denote force, moment, and the combined injury criteria.

## **DISCUSSION**

COMPARISON WITH OTHER STUDIES - Change in velocity and mean acceleration data compare well to previous studies. Using actual car-to-car rear impact collisions reported by Severy et al as a basis, Mertz and Patrick designed pulses for sled rear simulations that resulted in velocities of 4.0 and 6.7 m/s [2]. Average accelerations for the two velocities were 30.1 and 50.2 m/s<sup>2</sup>. These data parallel the present mean values of 32.4 m/s<sup>2</sup> for the 4.3 m/s (average of specimens 102 and 103) and 45.1 m/s<sup>2</sup> for the 6.8 m/s (mean of specimens 101, 104, 105).

Deng et al reported a peak extension angle of 48 degrees in an unembalmed cadaver tested at 1.9 m/s velocity [13]. Acknowledging that the test was done at approximately one-half to one-third value of the present velocities, the head extension angles in the present study appear reasonable. Maximum head extension angles reported by Mertz and Patrick (mean: 63 and 85 degrees for the 4.0 and 6.7 m/s) are somewhat lower than the current analysis. Differences in test conditions and specimen characteristics (embalmed male cadavers with 61 and 59 kg body weight, head weight 2.9 and 4.1 kg in the previous versus unembalmed small female and

large male cadavers in the present) may account for the discrepancy.

Head cg acceleration data obtained in the present study compared very favorably with the previous Mertz and Patrick's study. Lower-velocity tests in the current study yielded z accelerations in the range of 62.5 to 83.0 m/s<sup>2</sup> (Table A) and the previous study yielded for the equivalent test reported a range of 71.6 to 78.5 m/s<sup>2</sup>. Lower-velocity tests resulted in x accelerations ranging from 73.8 to 91.6 m/s<sup>2</sup> for the present study, compared to 71.6 to 78.5 m/s<sup>2</sup> for the previous study. For higher-velocity tests, the previous study reported maximum z acceleration values from 129.5 to 153.0 m/s<sup>2</sup>, compared to the present study values of 129.1 and 152.1 m/s<sup>2</sup>. The x accelerations for high-velocity tests in the present study ranged from 80.3 to 95.1 m/s<sup>2</sup>, compared to the previous study (88.3 to 104.0 m/s<sup>2</sup>). Thus, the cg head acceleration may be fairly independent of cadaver specimen characteristics including embalming conditions and size.

Peak shear and tension forces agree with the results from the previous study (245 to 400 N of shear and 187 to 311 N of tension at 4.0 m/s, and 271 to 444 N of shear and 418 to 502 N of tension at 6.7 m/s). For comparison, the present data at 6.8 m/s are: 257 to 525 N of shear and 672 to 904 N of tension; and at 4.3 m/s: 388 to 397 N of shear and 369 to 391 N of tension. Extension moment data also agree with this previous study wherein the torque ranged from 19.4 to 36.1 Nm (at 4.0 m/s) and 33.3 to 43.1 Nm (at 6.7 m/s) from two cadaver tests.

COMPARISON OF INJURIES - Injuries documented in this study parallels clinically detected lesion. For example, during surgical procedures intervertebral disc and facet joint injuries have been reported in patients sustaining rear-end crashes, although these specific joint-related injuries were not identified during routine clinical imaging techniques [14-17]. In addition, experimental animal studies have produced ruptures of the anterior ligaments during rear impact accelerations [18,19]. Previous human cadaver studies produced injuries to the disc and ligaments similar to those documented in the present study [20,21]. In the Mertz and Patrick study, they inferred "minor ligamentous damage between the third and fourth cervical vertebrae" based on posttest x-rays in one of the two cadavers Because detailed cryosectioning was not performed in this previous study, there may have been other soft-tissue injuries that went undetected. This is further evidenced by the present study wherein the cryosection analysis revealed injuries in four out of five specimens, whereas radiographic techniques revealed injuries in only two out of four specimens.

SAMPLE SIZE AND STATISTICS - The test matrix used in the present study did not include repeat tests (sample size greater than one under each condition, Table A). Consequently, commonly used processes of data analysis such as computations of mean and standard deviation (except for the applied rear impact acceleration pulse) were not adopted. This approach was employed for the following reasons. Data on the biomechanical responses to injury from intact human cadaver models are very limited in literature. To our knowledge, this is the only study that has attempted to document the resulting injuries to unembalmed intact human cadavers using imaging techniques capable of documenting hard and soft alterations to the headneck structures, determine the kinetics (kinematics), and evaluate injury criteria secondary to rear impact acceleration. It was also important to evaluate responses to small female and large male subjects under this mode, as differences have not been documented for these specific subject types.

EFFECTS OF EARLY COMPRESSIVE FORCE -Irrespective of impact velocity and other variables, variations in peak compressive forces were small (Table A). The compressive force develops early during the extension phase. Its development has been attributed to the straightening of the thoracic spine secondary to the interaction of the human torso with the seat back [22]. Using human cadaver cervical spine motion segment studies, Yang et al showed that the presence of the shear force with axial compressive force reduces the shear stiffness of the cervical spine [23]. They hypothesized that this combined shear and compressive mechanism can cause excessive stretch in the facet joint leading to neck pain and stated that "this hypothesis is also neurophysiologically sound."

LIMITATIONS - Certain limitations are inherent to the present model. Because of the use of human cadaver surrogates, active musculature responses are not included. Additional procedures may be necessary to account for modulations in the spinal activity secondary to partial or full muscle activation. Because the effects of such modulation are a topic of controversy in rear impact literature, the present analysis was divided into two categories, i.e., the initial extension phase and rebound phase. Based on previous studies, it may be appropriate to consider that the present biomechanical output is more realistic in the initial extension phase. Another factor is the use of a rigid seat. This procedure was used to obtain baseline data so the effects of seat yielding or flexibility are eliminated in the analysis. Additional studies are needed to include these types of variables.

It is obvious that any human cadaver study cannot directly address pain-related issues. The cadaver model is, however, uniquely valuable to examine mechanically induced pathologies such as fractures and soft-tissue ruptures. It is also very common in the literature to correlate trauma seen in cadaver studies to trauma that occurs to the living human [24-26]. It is with this premise that injury criteria are developed. However, most injury criteria have been developed for moderate-to-severe (AIS  $\geq$  2) injuries. Controversies surround the legitimate identification of low AIS injuries. Most of the time there is no radiographic evidence for these types of trauma. The present study incorporated the use of a cryomicrotome device to document "minor" injuries. Using this technique, it was possible to identify trauma that cannot be seen radiographically. It is, therefore, logical to take the same steps with minor injuries as have been taken with moderate and severe injuries. The major difficulty with this process for minor injuries is taking the next step of correlating soft-tissue ruptures with pain that could result in the living human. This subject requires further research.

# SUMMARY AND CONCLUSIONS

The following observations are obtained from the present study.

- 1. Five unembalmed intact human cadavers (specimens) were subjected to rear impact simulations at velocities of 4.3 or 6.8 m/s. Tests were conducted to examine head-neck injuries.
- 2. Instrumentation included: accelerometers and photographic targets for determining the kinetics (and kinematics) which included the forces and moments at the occipital condyles

- 3. Injuries were documented using x-ray, CT and cryomicrotomy techniques. One specimen did not show injury. However, injuries to joint-related structures were documented in the other four specimens.
- 4. Head cg accelerations, angular accelerations, forces and moments at occipital condyles agreed with literature and, in general, reached their respective maximum values in the extension phase.
- 5. Peak head cg accelerations in the z direction preceded the x accelerations. Peak angular acceleration was maximum for the specimen with the large body and head mass.
- 6. The peak compressive force at the occipital condyles preceded peak shear and tension forces. Regardless of other test variables (e.g., velocity, anthropometry), peak compressive forces (100 to 254 N) were lower than peak tension (361 to 904 N) and shear (257 to 525 N) forces at the occipital condyles. The maximum tension force appeared to depend more on velocity than the other two components.
- 7. Bending moments at the occipital condyles ranged from 22 to 33 Nm for low-velocity (4.3 m/s) and 33 to 47 Nm for high-velocity (6.8 m/s) tests.
- 8. The suggested neck injury criterion (NIC) limit  $(15 \text{ m}^2/\text{s}^2)$  was exceeded in all specimens.
- 9. Peak tension and compression forces did not exceed the proposed limits in all specimens. The risk of AIS  $\geq$  3 neck injury using N<sub>ij</sub> criteria was estimated to be zero in all specimens with the exception of one specimen (105) wherein it was 22 percent.
- 10. The risk of AIS  $\geq$  3 neck injury was estimated to be less than five percent in all specimens based on normalized tension ( $F_T$ ) and normalized extension ( $M_E$ ) criteria.
- 11. The risk of AIS  $\geq$  3 neck injury was estimated to be less than one percent in all specimens with the exception of one specimen (105) wherein it was 30 percent using the combined tension-extension criteria ( $N_{TE}$ ).

#### **ACKNOWLEDGMENTS**

This investigation was supported in part by Breed Technologies, The Ford Motor Company, The Lear Corporation, PHS CDC Grant R49CCR515433, TNO Crash Safety Center and the Department of Veterans Affairs Medical Research.

## REFERENCES

- Yoganandan N, Pintar, FA. Biomechanical Assessment of Whiplash. In: Frontiers in Head and Neck Trauma: Clinical and Biomechanical, N Yoganandan, FA Pintar, SJ Larson, and A Sances, eds. IOS Press, The Netherlands, 1998, pp 344-373.
- 2. Mertz HJ, Patrick LM. Investigation of the kinematics and kinetics of whiplash. 11th Stapp Car Crash Conf., Anaheim, CA, 1967.
- 3. McConville JT, Churchill TD, Kaleps I, Cuzzi J. Anthropometric relations of body and body segments moment of inertia. Wright-Patterson Air Force Base, 1980.
- 4. van den Kroonenberg A, Philippens M, Cappon H, Wismans J, Hell W, Langwieder K. Human head-neck response during low-speed rear end impacts. 42nd Stapp Car Crash Conf., Tempe, AZ, 1998.
- Wismans J, Van Oorschot H, Woltring HJ. Omni-directional human head-neck response.
   30th Stapp Car Crash Conf., San Diego, CA, 1986.
- Beier G, Schuck M, Schuller E, Spann W. Determination of physical data of the head. I. Centre of gravity and moments of inertia of human heads. IRCOBI. Birmingham, England, 1980.
- 7. Wismans J, Spenny CH. Head-neck response in frontal flexion. 28th Stapp Car Crash Conf., Chicago, IL, 1984.
- 8. Eppinger R, Sun E, Kuppa S, Saul R. Supplement: Development of Improved Injury Criteria for the Assessment of Advanced Automotive Restraint Systems II. Washington, DC: US DOT/National Highway Traffic Safety Administration, 1999 and 2000.
- 9. Federal Motor Vehicle Safety Standards, FMVSS 208, Code of Federal Regulations, Washington, DC, 2000.

- Dummy response limits for FMVSS 208 compliance testing. Annex 2 of the Alliance of Automobile Manufacturers submission to SNPRM, NHTSA Docket 99-6407-Notice 1, December 23, 1999.
- 11. Bostrom O, Haland Y, Svensson MY. Neck injury criterion (NIC) and its relevance to various possible injury mechanisms. In: Frontiers in Whiplash Trauma: Clinical and Biomechanical, N Yoganandan, FA Pintar, eds. IOS Press, The Netherlands, 2000, pp 457-467.
- Mertz HJ, Prasad P, Irwin AL. Injury risk for children and adults in frontal and rear collisions.
   41th Stapp Car Crash Conf., Lake Buena Vista, FL, 1997.
- 13. Deng B, Begeman PC, Yang KH, King AI, Anderst B, Tashman S. Kinematics of human cadaver cervical spine during low speed rear-end impacts. Impact biomechanics from head to foot. Detroit, MI, 1999.
- 14. Buonocore E, Hartman JT, Nelson CL. Cineradiograms of cervical spine in diagnosis of soft-tissue injuries. JAMA 198:143-147, 1966.
- 15. Janes JM, Hooshmand H. Severe extensionflexion injuries of the cervical spine. Mayo Clinic Proc. 40:353-368, 1965.
- Davis SJ, Teresi LM, Bradley WG, Ziemba MA, Bloze AD. Cervical spine hyperextension injuries. Radiology 180:245-251, 1991.
- 17. Howcroft AJ, Jenkins DH. Potentially fatal asphyxia following a minor injury to the cervical spine. J Bone Jt Surg. 59B:93-94, 1977.
- 18. MacNab J. Acceleration extension injuries of the cervical spine. In: The Spine, RH Rothman and FA Simeone, eds. Philadelphia, PA: WB Saunders, 1982, pp 647-660.

- 19. Wickstrom JK, Martinez JL, Rodriguez R, Haines DM. Hyperextension and hyperflexion injuries to the head and neck of primates. In: Neckache and Backache, ES Gurdjian, LM Thomas, eds. Springfield, IL: CC Thomas, 1970, pp 108-119.
- Clemens HJ, Burow K. Experimental investigation on injury mechanism of cervical spine at frontal and rear-frontal vehicle impacts. 16th Stapp Car Crash Conf., Detroit, MI, 1972.
- 21. Hu AS, Bean SP, Zimmerman RM. Response of belted dummy and cadaver to rear impact. 21st Stapp Car Crash Conf., New Orleans, LA, 1977.
- 22. McConnell WE, Howard RP, Van Poppel J, Krause R, Guzman HM, Bomar JB, Raddin JH, Benedict JV, Hatsell CP. Human head and neck kinematics after low velocity rear-end impacts understanding "whiplash." 39th Stapp Car Crash Conf., San Francisco, CA, 1995.
- 23. Yang KH, Begeman PC, Muser M, Niederer P, Walz F. On the role of cervical facet joints in rear end impact neck injury mechanisms. SAE, 1997.
- 24. Winklestein B, Myers B. Determinants of catastrophic neck injury. In: Frontiers in Head and Neck Trauma: Clinical and Biomechanical, N Yoganandan, FA Pintar, SJ Larson, and A Sances, eds. IOS Press, The Netherlands, 1998, pp 366-395.
- 25. Yoganandan N, Pintar FA, Larson, SJ and Sances A: Frontiers in Head and Neck Trauma: Clinical and Biomechanical, IOS Press, The Netherlands, 1998, 743 pp.
- Yoganandan N, Pintar FA. Frontiers in Whiplash Trauma: Clinical and Biomechanical, IOS Press, The Netherlands, 2000, 589 pp.

Table A: Summary of Data

Table A: Summary of Data	<del></del>					
Description	Phase					,
Subject Data						
Specimen identification number	N/A	101	102	103	104	105
Gender	N/A	Female	Female	Female	Male	Female
Height (m)	N/A	1.64	1.56	1.65	1.85	1.52
Weight (kg)	N/A	72.6	55.4	40.4	107.5	36.3
Neck data					- 200	
Neck*circumference (mm)	N/A	390	280	285	435	295
Head data		-				
AP Length (m)	N/A	0.181	0.17	0.19	0.19	0.175
Lateral Breadth (m)	N/A	0.15	0.15	0.145	0.16	0.15
Circumference (m)	N/A	0.559	0.535	0.56	0.605	0.54
Mass	N/A	4.29	3.9	4.2	5.17	3.95
Moment of Inertia (kg/m²)	N/A	0.0208	0.0165	0.021	0.029	0.0174
Test matrix	N/A					5.00
Velocity (m/s)	N/A	6.89	4.14	4.41	6.58	6.81
Mean Acceleration. (m/sec/sec)	N/A	45.1	32.4	32.4	46.1	44.1
Pulse Width (ms)	N/A	151	128	137	152	159
Cushion Use	N/A	No	No	Yes	Yes	Yes
X-ray data					-	
Orbit x coordinate (mm)	N/A	81	70	76	95	69
Orbit a coordinate (mm)	N/A	0	0	0	0	0
OC x coordinate (mm)	N/A	-3	-10	-12	5	2
OC z coordinate (mm)	N/A	-22	-16	-6	-22	-7
T1 x coordinate (mm)	N/A	-64	-69	-62	-72	-58
T1 z coordinate (mm)	N/A	0	0	0	0 ,	0
Peak T1 accelerations						
Positive x-acceleration (m/sec/sec)	Extension	132.8	82.9	103.6	101.1	95.9
Time of occurrence (ms)	Extension	96	105	81	77	82
Negative x-acceleration (m/sec/sec)	Extension	-24.0	-19.9	-7.6	0.0	-21.6
Time of occurrence (ms)	Extension	185	184	201	0	95
Positive z-acceleration (m/sec/sec)	Extension	42.7	20.4	75.6	79.8	67.6
Time of occurrence (ms)	Extension		110	94	197	46
Negative z-acceleration (m/sec/sec)	Extension	-50.3	-76.9	-14.0	-65.7	-59.6
Time of occurrence (ms)	Extension	77	174	134	169	105
Positive x-acceleration (m/sec/sec)	Rebound	40.8	62.3	60.1	28.9	28.4
Time of occurrence (ms)	Rebound	209	216	209	253	209
Negative x-acceleration (m/sec/sec)	Rebound	-45.0	-10.7	2.3	-20.7	-27.8
Time of occurrence (ms)	Rebound		518	454	547	338
Positive z-acceleration (m/sec/sec)	Rebound		20.2	49.8	49.6	13.9
Time of occurrence (ms)	Rebound	191	219	228	316	221
Negative z-acceleration (m/sec/sec)	Rebound	<del></del>	-38.8	-26.8	-36.2	-25.2
Time of occurrence (ms)	Rebound	<del></del>	519	522	339	318

Table A: Continued

Table A: Continued	- ·					
Description	Phase	Test ID Number				
Specimen identification number	N/A	101	102	103	104	105
Peak head extension angle						
Extension angle (deg)	Extension	143	149	137	123	123
Time of occurrence (ms)=length of extension phase	Extension	192	216	203	196	179
Head displacements			Transfer			
Anteroposterior (m)	Extension	0.09	0.16	0.08	0.10	0.08
Inferior to superior (m)	Extension	0.03	0.03	0.02	0.02	0.01
Superior to inferior (m)	Extension	0.04	0.05	0.09	0.09	0.10
Head CG accelerations		and warried to make	e to a majora,			4 1 1 1 2 2 3 2 2 3
Positive x (m/sec/sec)	Extension	80.3	61.6	73.8	86.5	95.1
Time of occurrence (ms)	Extension	190	191	198	187	185
Negative x (m/sec/sec)	Extension	-81.1	-82.6	-86.0	-75.5	-80.0
Time of occurrence (ms)	Extension	159	164	155	155	156
Positive z (m/sec/sec)	Extension	48.4	27.0	9.7	26.6	27.3
Time of occurrence (ms)	Extension	52	41	55	66	65
Negative z (m/sec/sec)	Extension	-149.1	-62.5	-83.0	-129.1	-152.1
Time of occurrence (ms)	Extension	149	212	95	158	158
Positive x (m/sec/sec)	Rebound	84.5	91.6	65.9	61.8	85.8
Time of occurrence (ms)	Rebound	310	225	218	210	200
Negative x (m/sec/sec)	Rebound	-76.9	-31.6	-7.1	-45.6	-50.1
Time of occurrence (ms)	Rebound	534	547	399	515	491
Positive z (m/sec/sec)	Rebound	59.3	-14.9	-16.1	3.9	0.8
Time of occurrence (ms)	Rebound	304	432	329	529	529
Negative z (m/sec/sec)	Rebound	-129.1	-53.2	-69.7	-77.6	-86.4
Time of occurrence (ms)	Rebound	286	216	221	210	208
Head angular accelerations					210	200
Head angular acceleration (rad/sec/sec)	Extension	919	777	1090	1200	590
Time of occurrence (ms)	Extension	109	90	97	99	40
Head angular acceleration (rad/sec/sec)	Rebound	1310	122	4	646	370
Time of occurrence (ms)	Rebound	308	284	221	448	460
Forces at occipital condyles				221	110	700
Shear force (N)	Extension	345	268	388	525	257
Time of occurrence (ms)	Extension	181	198	199	191	170
Compressive force (N)	Extension	-203	-100	-119	-132	-254
Time of occurrence (ms)	Extension	50	35	53	61	48
Tensile force (N)	Extension	723	391	369	904	672
Time of occurrence (ms)	Extension	149	211	200	156	165
Shear force (N)	Rebound	378	397	335	471	183
Time of occurrence (ms)	Rebound	310	224	222	201	192
Tensile force (N)	Rebound	620	329	351	627	330
Time of occurrence (ms)	Rebound	285	224	222	207	
Bending moment at occipital condyles			-4 F	LLL	207	200
Extension moment (Nm)	Extension	40.0	22.0	33.5	46.6	
Time of occurrence (ms)	Extension	184	191	200	197	32.7
Extension moment (Nm)	Rebound	19.9	24.0	200	17/	173
Time of occurrence (ms)	Rebound	259	222	-	-	8.0
			444			209

Table A: Continued

Description	Phase	Test ID Number				
Specimen identification number	N/A	101	102	103	104	105
Neck injury criteria	Modella.			1 1457451		
Neck injury criteria based on FMVSS 208 [9,10]	*11-12X-2-15					
Out-of-position peak tension criterion (Table 1)	Extension	0.35	0.19	0.18	0.23	0.32
Out-of-position peak compression criterion, table 1	Extension	0.08	0.04	0.03	0.03	0.12
N <sub>ii</sub> out-of-position occupant tension-extension	Extension	0.60	0.30	0.45	0.21	1.30
Time of occurrence (ms)	Extension	181	189	200	196	155
AIS 3+ injury risk (%)	Extension	0	0	0	0	22
Neck injury criterion [11]						
NIC value (m <sup>2</sup> /s <sup>2</sup> )	Extension	37.0	19.2	25.8	25.7	23.1
Neck injury criteria [12]		4-18-55		100		raistas, t
Peak tension value (Table 2) exceeded (Y/N)	Extension	N	N	N	N	N
Peak extension value (Table 2) exceeded (Y/N)	Extension	Y	N	Y	N	Y
Normalized peak tension (F <sub>T</sub> )	Extension	0.43	0.23	0.22	0.28	0.40
AIS 3+ injury risk (%)	Extension	0.1	0.0	0.0	0.0	0.1
Normalized peak moment (M <sub>E</sub> )	Extension	1.59	0.89	1.33	0.70	1.30
AIS 3+ injury risk (%)	Extension	4	0	2	0	3
Combined tension-extension (N <sub>TE</sub> )	Extension	1.16	0.71	1.02	0.57	2.27
Time of occurrence (ms)	Extension	186	200	200	195	155
AIS 3+ injury risk (%)	Extension	1	1	1	1	30

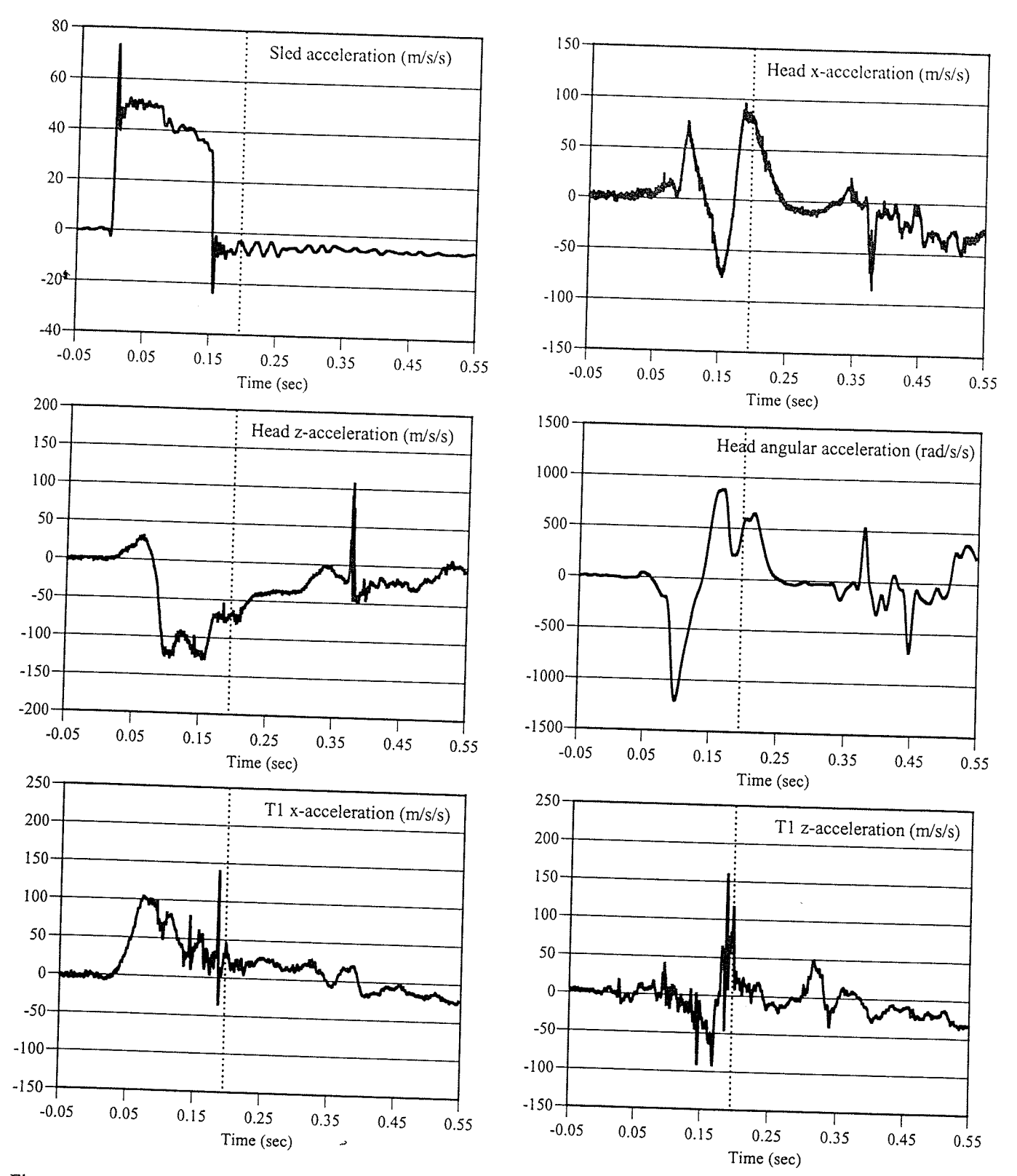


Figure A1: Time plots for sled pulse, head cg x and z accelerations, head angular acceleration, and T1 x and z accelerations for specimen 104. Data are split into extension and rebound phases by a vertical dotted line in each graph. The extension phase ended when the head was in maximum angular extension.

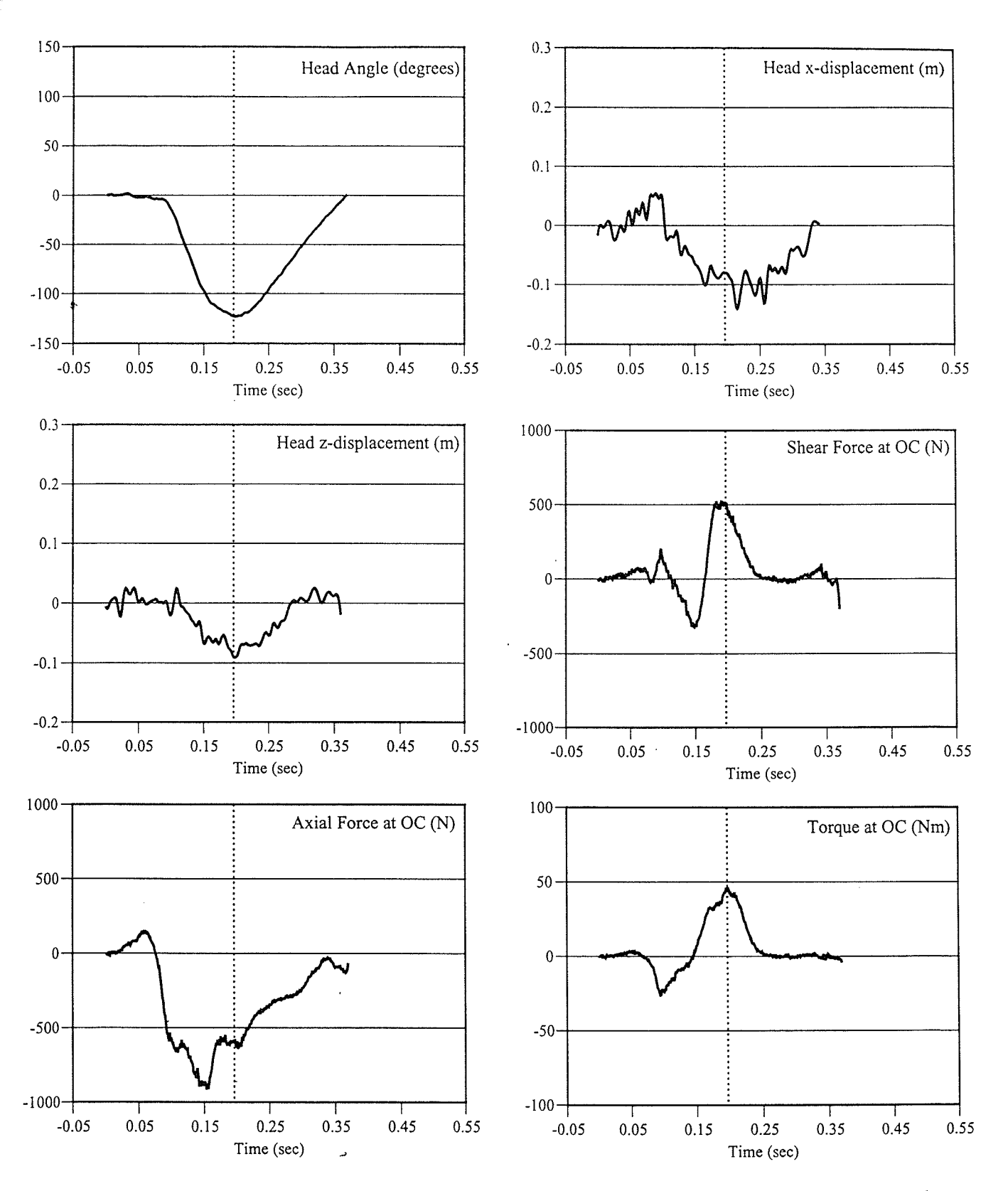


Figure A2: Time plots for head extension angle, head x and z displacements, and axial force, shear force, and torque at the occipital condyles for specimen 104. Data are split into extension and rebound phases by a vertical dotted line in each graph. The extension phase ended when the head was in maximum angular extension.

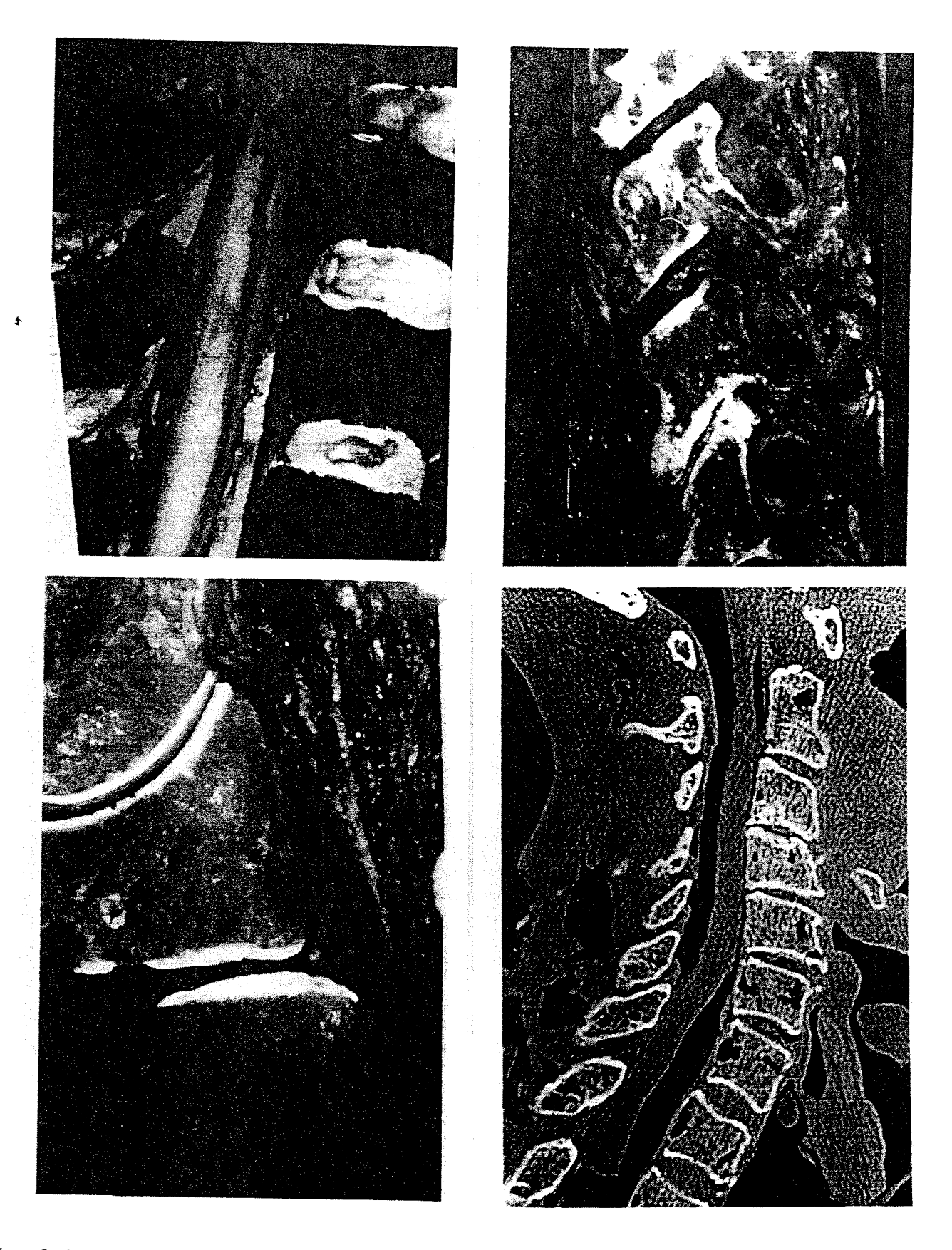


Figure 5: Clockwise from top left: Cryomicrotome section of specimen 103 illustrating the tear of the ligamentum flavum at C6-C7; cryomicrotome section of specimen 104 demonstrating the dastasis (widening) of the C5-C6 facet joint; sagittal CT image of specimen 105 illustrating chip fracture of the C5 body; cryomicrotome section of specimen 105 demonstrating blood in the C1-C2 joint.